Multibeam Antennas With Polarization and Angle Diversity

Darko Popovic and Zoya Popovic, *Fellow, IEEE*

***Abstract*—A 10-GHz discrete cylindrical lens array with multiple beams is designed and characterized as a receiving angle-diversity array for wireless communications in a multipath environment. The array also has dual-orthogonal polarization and therefore built-in polarization diversity. The array is designed for wide-angle scanning between −45° and 45°and measured scanning patterns are presented. The polarization isolation between the two channels is about 30 dB at boresite and about 10 dB for a 30° scan angle. The addition of the lens array at the very front end of a link shows significant reduction of multipath fading peak-to-null ratio.**

***Index Terms*—Antenna arrays, diversity methods, multibeam antennas, polarization.**

I. Introduction

THE BENEFITS of different types of diversity in wireless communications have been known since the first mobile radio systems [1]. Spatial [2]–[4], polarization [2], [4], [5], angle [2], [3], or frequency diversity have been used or proposed to improve signal-to-noise ratio, bit-error rate, channel capacity, and power savings in a mobile link. In this paper, we examine the use of more than one type of diversity in the same front-end antenna array—in specific, polarization and angle diversity. The antenna is a discrete lens array, inherently having multiple beams with a single spatial feed and designed to have dual linear polarization. The lens array is planar and lightweight, fabricated using standard printed circuit technology. In this approach, a standard N-element antenna array followed by a feed network is replaced by a discrete lens array in which N array element pairs perform a Fourier transform operation on the incoming wave front, and $M < N$ receivers are placed on a focal surface sampling this image. The lens array can include integrated amplifiers in each element and different lenses have been demonstrated for spatially-fed transmit-receive arrays at *X* [6] and *Ka* bands [7]. In active discrete lenses with distributed amplifiers, in transmission the effective radiated power (ERP) is increased with accompanied increase in reliability and efficiency, while in reception the dynamic range is improved as the low-noise amplifier (LNA) noises add incoherently, while the signal adds coherently. A lens array was also successfully integrated with an analog holographic optical processor in an optically-smart antenna array [8]. The lens array as the front end of a system performs spatial separation of the input waves, which enables simplified subsequent processing. The front-end processing benefits when using a discrete lens in an adaptive array, as applied to interference and multipath propagation, were investigated in [9].

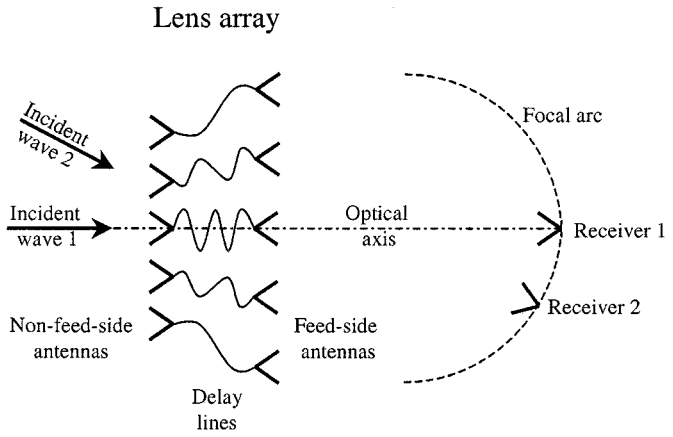

Fig. 1. A lens antenna array consists of two interconnected antenna arrays. The unit element of the lens array is a pair of antennas, connected with a delay line. The length of the delay varies across the face of the array such that an incident plane wave is focused onto a focal point in the near field on the feed side of the array. Plane waves incident on the nonfeed side of the array from different directions are focused onto different points on the focal surface, where receiving antennas and circuitry are placed to sample the image.

A schematic of a lens array is shown in Fig. 1 and is here discussed in receive mode, although the lens is reciprocal and can also be used in a transmitter. The unit element of the lens array consists of two antennas, interconnected with a delay line [10]. The length of the delay varies across the array such that an incident plane wave is focused onto a focal point in the near field on the feed side of the array in Fig. 1. Plane waves incident from different directions are focused onto different points on the focal surface, where receiving antennas and circuitry are placed to sample the image, which is a discrete Fourier transform of the incoming wavefront. The discrete lens has improved focusing properties over some dielectric lenses and reflector antennas, as it can be designed for low-sidelobe levels at large-steering angles [10]. Multiple receivers correspond to multiple antenna radiation pattern beams, enabling beam steering and beam forming with no microwave phase shifters. In a multipath environment, each of the reflected waves is focused onto a different receiver, giving angle diversity.

In this paper, a lens array is used due to its inherent angle diversity property, but the antenna elements are also designed to have dual orthogonal polarization, providing polarization diversity. In the next section, the design and characterization of a

Manuscript received June 21, 2001; revised October 25, 2001. This work was supported by the National Science Foundation Wireless Initiative under Grants ECS-9979355 and ECS-9979400.

The authors are with the Department of Electrical and Computer Engineering, University of Colorado, Boulder, CO 80309 USA (e-mail: zoya@colorado.edu).

Publisher Item Identifier S 0018-926X(02)05443-1.

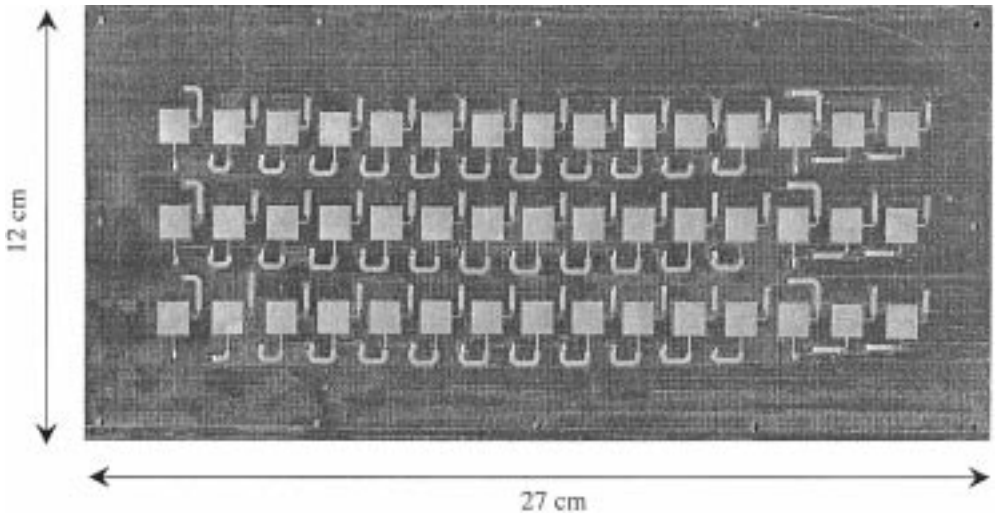

Fig. 2. Photograph of one side of a 45-element 10-GHz cylindrical lens antenna array shows the patch antenna elements with dual-polarization feed lines and the microstrip delay lines connected with via holes to orthogonally polarized patches on the other side of the two-layer lens array.

10-GHz dual-polarized cylindrical lens are described. The lens is placed in a controlled multipath environment and the reduction of multipath fading effects is shown experimentally.

II. Multibeam Lens Antenna Array—Design and Performance

The lens array designed for this study is a cylindrical 45-element array with three 15-element rows, which serve to provide a fan-shaped beam in the vertical direction. The photograph of one side of the lens, Fig. 2, shows the patch antenna elements with dual-polarization feed lines and the microstrip delay lines connected with via holes to orthogonally polarized patches on the other side of the two-layer lens array. Orthogonal polarization between the nonfeed and feed sides of the lens improves the isolation between the two sides. A single element of the lens is schematically shown in Fig. 3. It consists of a pair of dual-polarized patch antennas printed on two microstrip substrates with a common ground plane. The substrates used in this design have a relative permittivity of 2.5 and are 0.508 mm thick. The patches are designed to be resonant at 10 GHz are 9.1-mm squares, and the feed points are matched to 50-ohm feed lines with quarter wave 112-ohm matching sections. Each feed line is connected with a via to the corresponding orthogonally polarized feed line of the patch on the other side of the ground plane. The vias are metal posts 0.8 mm in diameter.

The 2-port S-parameters of the single element of the array were measured using an HP8510 Network Analyzer with a 3.5-mm coaxial calibration and are compared to simulations obtained using Zeland's IE3D method of moments (MoM) software, as shown in Fig. 4. From these measurements, it can be seen that the isolation between the two ports of the patch is about 35 dB at resonance, which implies that the two polarization channels are practically independent and can provide polarization diversity. The measured E- and H-plane radiation patterns of the single element in both polarizations are shown in Fig. 5. The asymmetry in the radiation patterns is clearly seen to be due to the feed lines, as the patterns from one feed are almost the same as those for the other, but flipped by

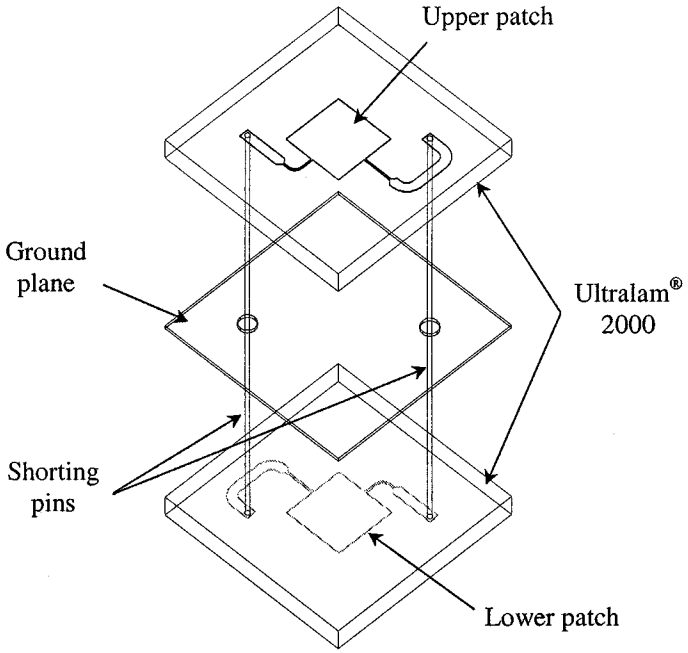

Fig. 3. A single element of the lens consists of a pair of dual-polarized patch antennas printed on two microstrip substrates with a common ground plane. The substrates have a relative permittivity of 2.5 and are 0.508 mm thick. The 10-GHz patches are 9.1-mm squares, and the feed points are matched to 50-Ω feed lines with quarter wave 112-Ω matching sections. Each feed line is connected with a via to the corresponding orthogonally polarized feed line of the patch on the other side of the ground plane.

180°. The axial ratio at the two ports is about 30 dB as shown in Fig. 6 and the two feeds are seen to be in perfect quadrature, i.e., the peak of one polarization coincides with the null of the other.

The element spacing in the array from Fig. 2 is half of a free space wavelength in one plane and 0.85λ in the other plane. The delay lines and the positions of the antenna elements at the feed side with respect to the ones at the nonfeed side are used as the design variables. They are calculated to give two perfect focal points located at the angles $\theta_0 = \pm 45°$. The design equations are given in [10]. Since perfect focusing exists only

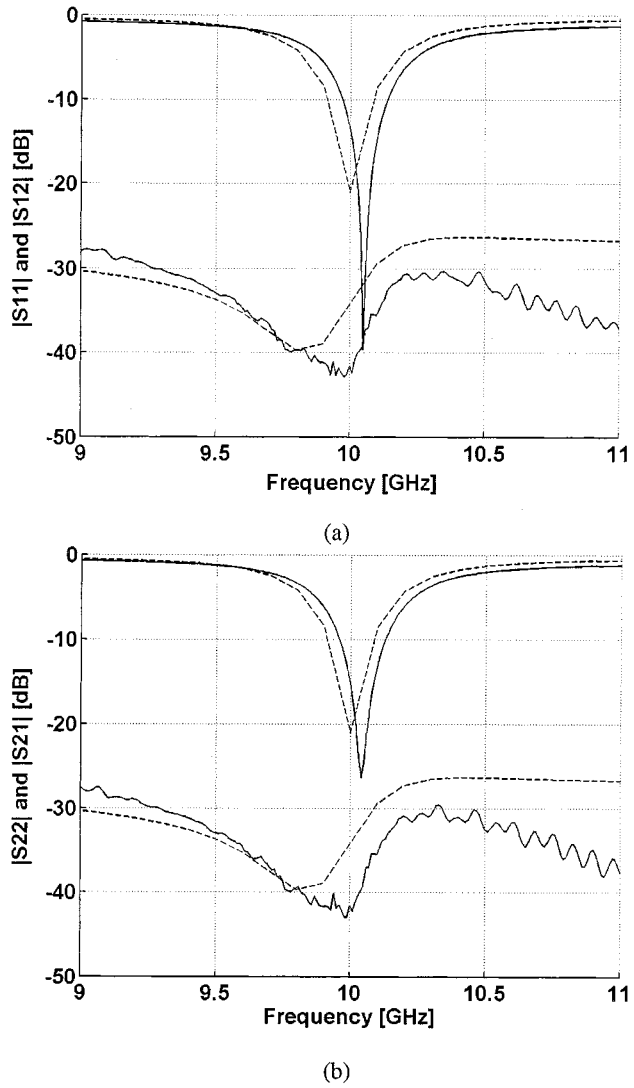

Fig. 4. Measured (solid line) and simulated (dashed line) two-port unit cell s-parameters, where the ports correspond to orthogonally polarized feeds.

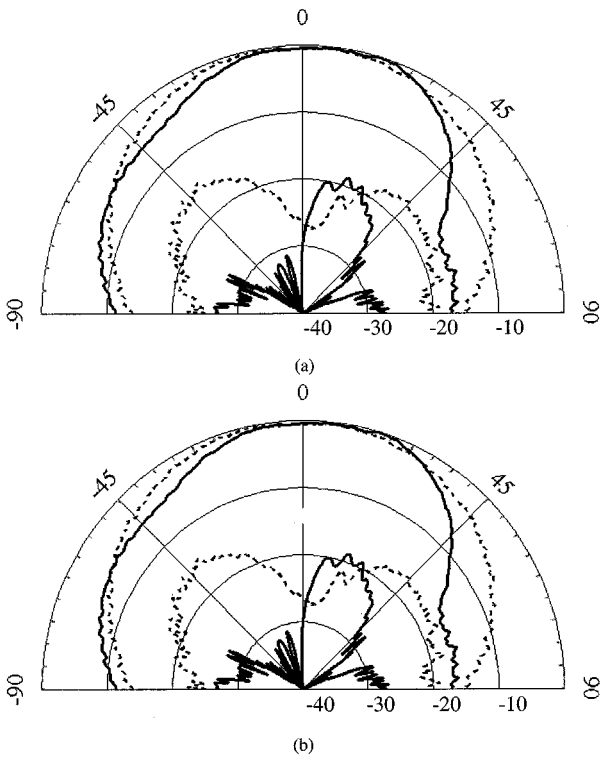

Fig. 5. Measured element E-plane (solid) and H-plane (dahed) co- and cross-polarized radiation patterns for the two orthogonally polarized ports, (a) and (b).

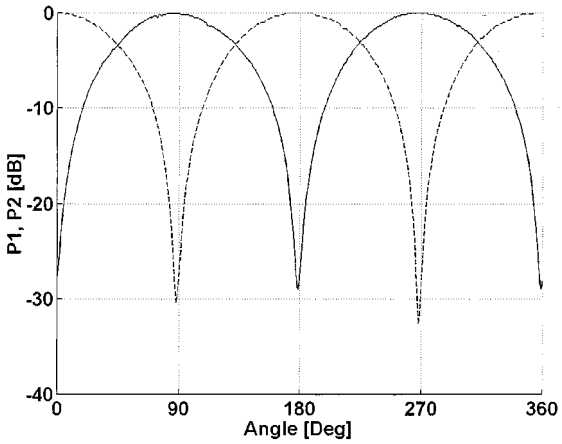

Fig. 6. Measured axial ratio of array element for the two orthogonally polarized feeds. The solid and dashed lines are the measured relative powers received at the two ports of the element as the transmitting horn polarization is rotated.

for the plane waves incident at $+45^\circ$ and -45°, for any other angle of incidence the path-length errors are present, which in turn degrades the radiation pattern. As described in [10], these errors can be significantly reduced by "refocusing." Therefore, the feeds are not positioned at the focal arc with a constant radius equal to the focal distance, but rather at the optimum focal arc which minimizes the path-length errors. The difference in length between the longest and shortest delay line is 0.35λ, the focal distance-to-diameter ratio is $F/D = 1.5$, with $F = 324$ mm.

The lens was characterized in an anechoic chamber using the setup shown in Fig. 7. A standard gain horn antenna is copolarized with the nonfeed side of the lens array and used as a transmitter in the measurements. For measuring radiation patterns corresponding to different beams of the multibeam lens, the lens is rotated and power detected at one receiver at a time. Linearly polarized horn antennas are used as the receiver antennas, but the same patches as the array elements can be alternatively used. The resulting normalized radiation patterns for receivers positioned between -45° and $+45^\circ$ along the focal arc are shown in Fig. 8. As the scan angle increases, the beam widens and the first sidelobe increases. The maximum received power for each of the patterns in Fig. 8 varies by about 1.5 dB in the range of scan angles and is plotted in Fig. 9 along with the half-power beamwidth of the main lobes. The asymmetry in the maximum received power behavior is due to the asymmetry in the radiation pattern of the patch element as seen from Fig. 5. In this range of scan angles, the first sidelobe level varies from -15 dB at 0° to -9 dB at 45°.

Two parameters that affect the shape of the lens far-field pattern are the path-length error for feed positions that are not at the perfect focal points and the amplitude distribution across

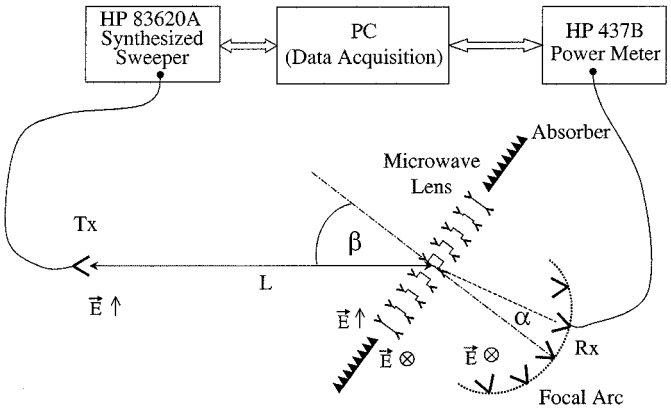

Fig. 7. Sketch of measurement setup used to characterize the lens array. A standard-gain linearly polarized far-field horn antenna is used as a transmitter and another horn antenna is used at the receive port.

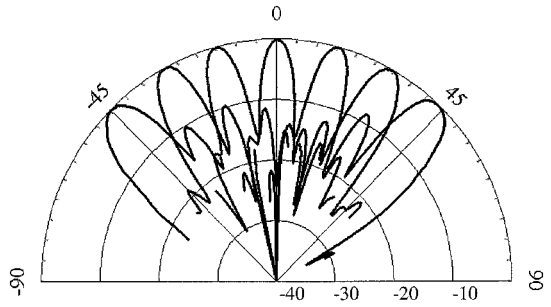

Fig. 8. Measured normalized multibeam patterns for receivers (or transmitters) positioned at points along the focal arc corresponding to beams at $-45°$, $-30°$, $-15°$, $0°$, $15°$, $30°$, and $45°$. Sidelobe levels for a beam steered to $-45°$ are shown in more detail as compared to simulations in Fig. 11.

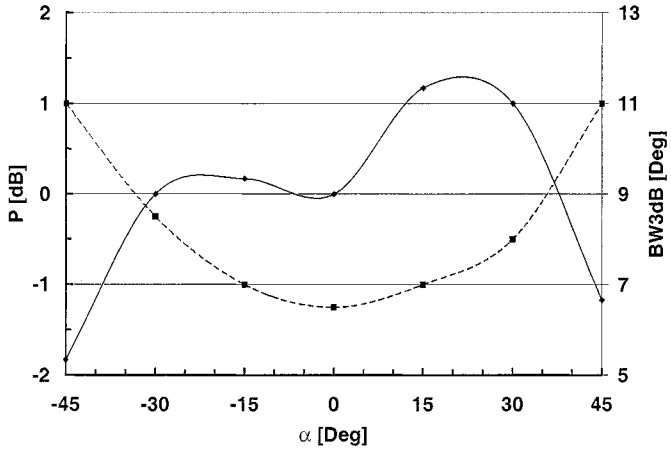

Fig. 9. Measured received power (solid line) and half-power beamwidth (dashed line) as the receiver is moved along the lens focal arc, normalized to the power level received on the optical axis.

the feed-side elements due to the spatial feed (this is easy to understand in transmission mode). Calculated lens array radiation patterns with the corresponding path-length errors and amplitude distributions, for beams at boresite and steered to $-45°$ are presented in Fig. 10(a) and (b), respectively. Dashed lines present the case when the amplitude distribution is uniform and the receiving antennas are positioned at a distance F from the center of the lens array. Solid lines present the case with the actual nonuniform amplitude distribution and with the receiving

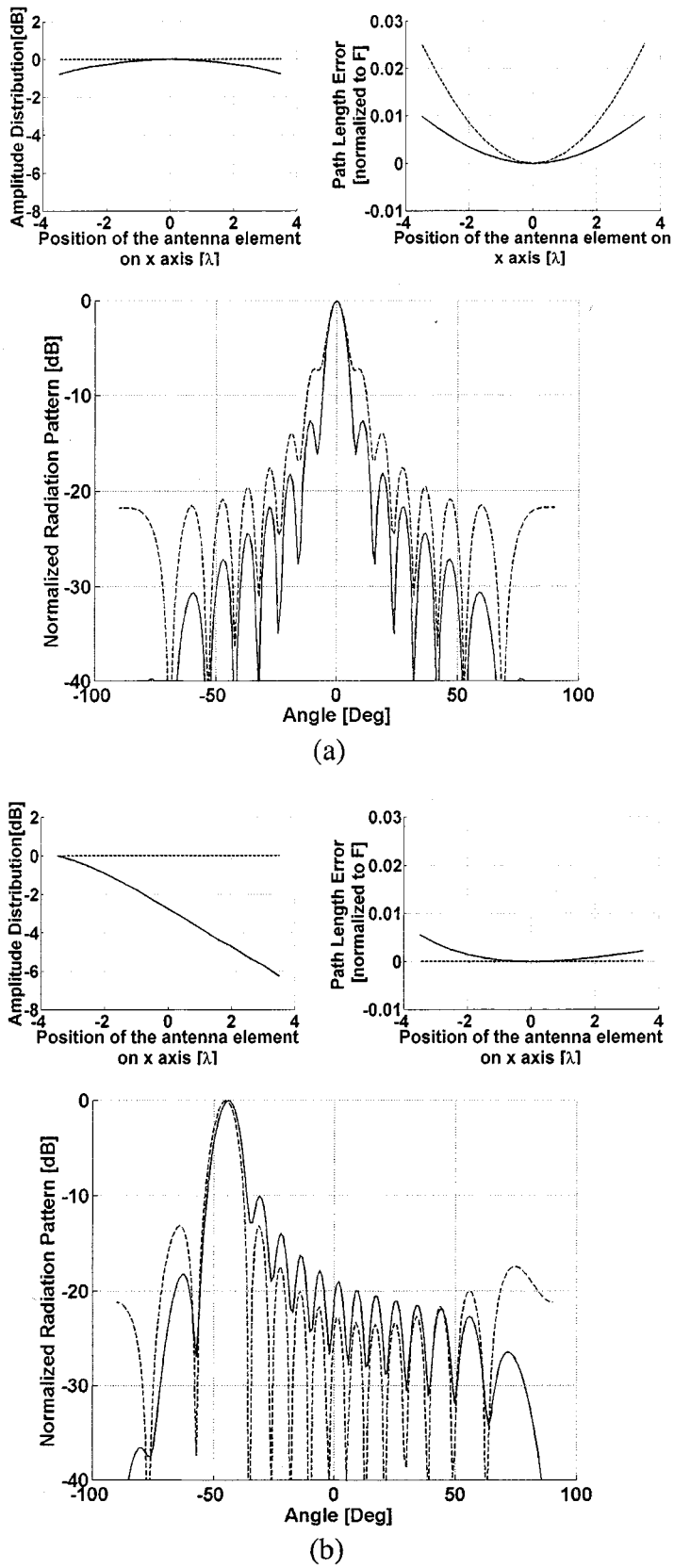

Fig. 10. Calculated lens array radiation patterns with the corresponding amplitude distributions and path-length errors, for a beam at boresite (a), and steered to $-45°$ (b). Dashed lines represent the case for uniform amplitude distribution and the receiving antenna at a distance F from the lens array. Solid lines represent the case with the actual amplitude distribution and the receiving antenna at the optimal focal arc.

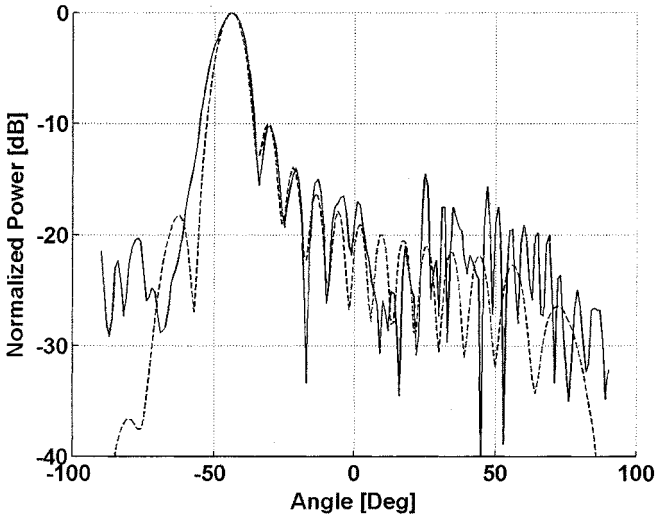

Fig. 11. Calculated (dashed) and measured (solid) lens array radiation patterns for a beam steered to -45°.

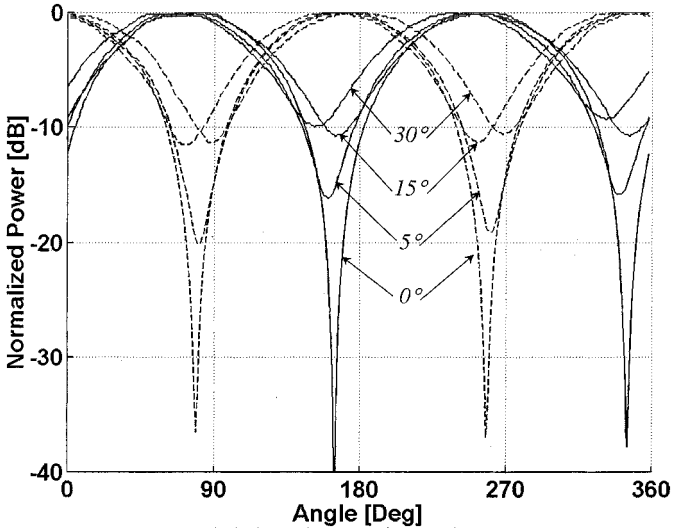

Fig. 12. Measured polarization properties for the two polarization states of the lens for four scan angles (0,° 5°, 15°, and 30°) as the transmitting horn polarization is rotated.

antennas positioned along the optimal focal arc. The amplitude distributions and the path-length errors are calculated for the 15 antenna elements in the middle row of the antenna array. The x-axis in these graphs is the position of the antenna elements along the row with the origin located at the center of the lens array. An improvement of more then 5 dB in the first sidelobe level is achieved by refocusing for the beam at boresite, as shown in Fig. 10(a). For the beam steered to -45°, nonoptimal amplitude distribution contributes to an increase in the first sidelobe level. The agreement between calculated and measured radiation patterns is shown in Fig. 11 for a beam steered to -45°. For other scan angles, the agreement between calculated and measured radiation patterns is either better or comparable to the case presented in Fig. 11. The axial ratios of the two-orthogonal polarizations of the lens were measured at 10 GHz as a function of scan angle, and the results are shown in Fig. 12 for four different scan angles. In this measurement dual-polarized patch antennas as the ones in Fig. 3 are used at the receive port and both polarizations are measured simultaneously. The axial ratio degrades with increased scan angle and the two polarizations become more coupled, which can be noticed not only in the level of the cross-polarized signal, but also in the relative position of the nulls and peaks for the two polarization states. Note that as the scan angle is increased, the beamwidth broadens, the sidelobe level increases, and the polarization isolation degrades. Because of these trends for higher angles, we chose to optimize the lens design for the two beams at 45° and -45°, not the beam on boresite (0°).

Since the lens is intended to be the receiving antenna, it is important to minimize the loss in the antennas, feed lines, and spatial feed, as any loss before the LNAs has a detrimental effect on the noise figure. In order to obtain an indication of lens efficiency, "thru" measurements are performed in a 4-m-long anechoic chamber. The transmitting and the receiving horn antennas are connected to a synthesized sweeper and power meter, respectively. The reference (0-dB) level is determined by copolarizing the antennas and measuring the line-of-sight received power level for a given transmitted power. The lens array is then inserted in front of the receiving horn antenna. It was mentioned before that the lens array has built-in polarization isolation and therefore the receiving horn antenna has to be rotated by 90°. Two sets of thru measurements are discussed. In the first one, the receiving antenna is positioned at the focal distance, $F = 324$ mm, and in the second, the feed is moved to the position which minimizes the path-length error (at the optimum focal arc), which for a beam at boresite is equal to $G = 458$ mm. The distance between the transmitter and the lens array is 3.6 m. The lens array is mounted in an absorber aperture of the same size as the lens and the total absorber size is a square 60 cm on the side. The measurements were made for the system that is calibrated in two ways: without the absorber and through the aperture in the absorber. Table I summarizes these measurements for both polarization states of the lens.

This measurement tells us how efficient our system is in collecting the RF power relative to a system without the lens array. Since the effective area is increased with the presence of the lens array we would expect to be able to collect more power. However, the results in Table I show us that the total received power is in most cases below the level that we would receive using the receiver antenna alone. That is due to the loss in the system where the main contributor is the spill over loss. This loss can be significantly reduced if we design the lens array and the receiving antenna as a system. In the case of the cylindrical lens, which we are considering, that would lead us to a receiver in the form of an antenna array with several antenna elements positioned in the vertical plane where most of the power gets focused. Calculations show that the thru measurement would result in 8-dB improvement in case of a 15-by-15-element lens array with the same antenna elements and the lens parameters as the 45-element lens array presented here. It is important to note here one advantage of the discrete-lens arrays over multibeam or phased arrays. Multibeam array feeds for large number of beams and elements become very complex and contribute to an increase in

TABLE I
THRU MEASUREMENTS OF THE LENS ARRAY FOR FEED LOCATED AT FOCAL DISTANCE AND AT THE OPTIMUM FOCAL ARC FOR THE TWO POLARIZATIONS. THE MEASUREMENTS WERE DONE USING TWO DIFFERENT CALIBRATIONS (ONE WITHOUT AND ONE WITH AN ABSORBER APERTURE)

Polarization of Tx/Rx	Feed distance [mm]	Relative received power (w/o aperture)	Relative received power (with aperture)
Tx – V, Rx – H	F=324	-2.2 (dB)	-0.7 (dB)
Tx – V, Rx – H	G=458	-4 (dB)	-3.9 (dB)
Tx – H, Rx – V	F=324	-1.5 (dB)	0.9 (dB)
Tx – H, Rx – V	G=458	-3.5 (dB)	-2.9 (dB)

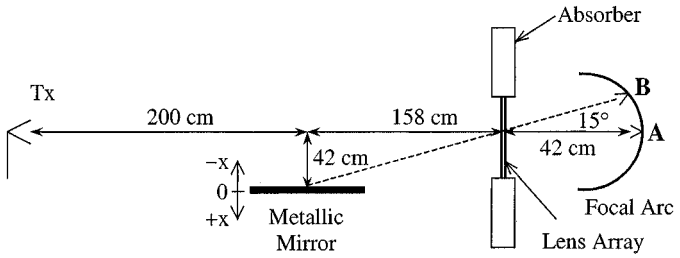

Fig. 13. Multipath measurement setup with a single 15×15 wavelength reflector which is translated by three wavelengths in the x direction. The $x = 0$ reference level corresponds to the second null in the lens radiation pattern, as shown in Fig. 10(a).

cost and losses. In lenses, however, the feed network complexity and losses scale favorably.

III. MULTIPATH FADING REDUCTION

Based on the characterization of the array shown in the previous section, we expect to see improvements in a link in a multipath fading environment when the lens is used at the front end. In order to test this, the lens is placed in a simple controllable multipath environment consisting of a single metal reflector in an anechoic chamber, as shown schematically in Fig. 13. The reflector is 15×15 free-space wavelengths large and is translated in the x direction over three free-space wavelengths. The reflector is positioned so that at $x = 0$, the reflected wave from the transmitting horn falls into the second null of the lens antenna pattern for a receiver on the optical axis (receiver A in Fig. 13), consistent with the radiation pattern from Fig. 8. In the first set of measurements, Fig. 13, the received power in a line-of-sight link between the transmitting horn antenna and the receiving patch, with no lens array present, was measured without the presence of the mirror, and then as the mirror was translated in the x direction. The power at the input of the transmitting horn is 500 mW. The straight horizontal lines on the plots in Fig. 14(a) and (b) are the measured power for the direct link only, without the reflector present. When the reflector is added, there is a standing wave behavior typical of a multipath environment. When the lens array is placed in front of the receiving antenna, the multipath peak-to-null ratio is significantly reduced, partly due to the gain of the array, and partly due to the built-in angle diversity.

When the receiver is positioned at point B on the focal arc corresponding to a beam at -15°, the reference level of the received signal without the mirror is 30 dB below the reference

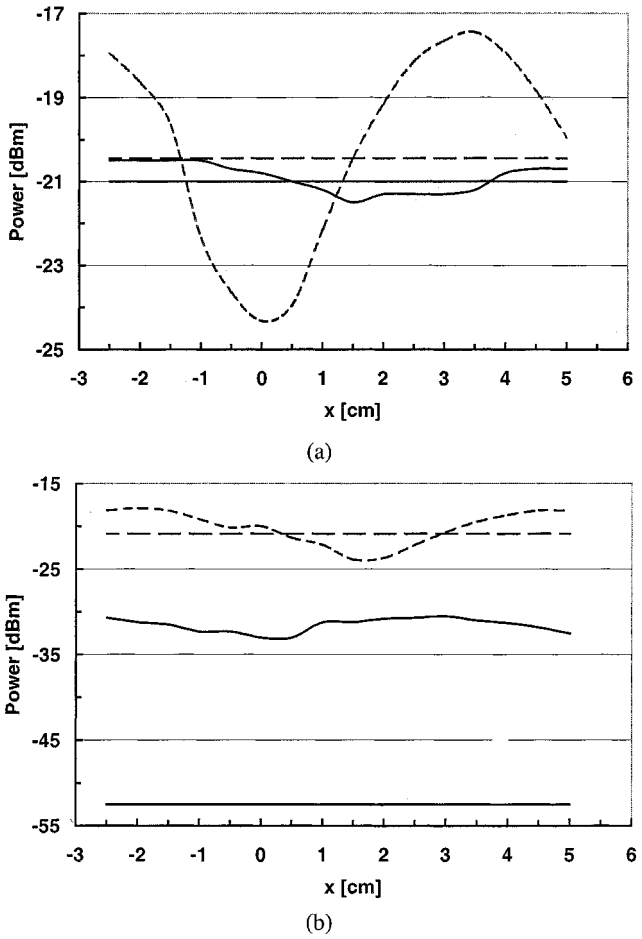

Fig. 14. Measured received copolarized power in the presence of a reflector without lens in link (dashed line) and with the lens added at the front end of the receiver (solid line). The receiver is positioned for a beam at 0° (a) and -15° (b). The straight lines show the reference power levels received with no reflector (no multipath) in the link, for 500-mW input power to the transmitting horn antenna in Fig. 12.

level measured with the feed on optical axis (straight solid lines in Fig. 14(a) and (b). This agrees well with the second null at 15° in the radiation pattern in Fig. 8, which is about 30 dB below the main beam. When the metallic mirror is placed in the experiment, the level of the signal is on average raised by 20-dB compared to the reference power level measured without the mirror [solid lines in Fig. 14(b)]. Therefore, the reflected multipath signal is spatially separated from the direct signal and the two are received separately and can subsequently be combined to obtain an increased signal level.

IV. Discussion

This paper describes a front-end discrete lens antenna array as it applies to wireless communications with more than one diversity type. The lens array is shown to be a multibeam array that can be designed to have low loss for large numbers of elements for two orthogonal well-isolated (30-dB) polarizations. In a transmitter, where each element can have a power amplifier, the powers will add coherently. In a receiver application where low-noise amplifiers are integrated in each antenna element, the noises add incoherently, while the signals add coherently at the receivers along the focal arc, therefore increasing the RF dynamic range by $10 \log N$. High output power with good efficiency in transmit mode, and low noise figure with good dynamic range in receive mode are crucial issues in wireless systems effectively addressed by active lens arrays.

The lens array can simultaneously receive beams incident from different directions, allowing for angle diversity in multipath communication channels. New multipath multi-antenna virtual space channel models [11] in which the channel is modeled with fixed spatial basis functions defined by fixed virtual angles have been introduced recently. These "virtual" angles each correspond to a single receiver on the focal surface of the lens. The spatial (angle) diversity afforded by the channel, which critically affects outage capacity, can in this case be taken explicitly into account, with excellent correspondence to physical reality. The lens and channel, modeled with virtual space theory, would provide a natural approach to receivers with low-complexity processing, but also to spatially selective signaling at the transmitter end, an area that has recently been of great interest to communication system engineers.

The lens array is a multibeam array with a single spatial feed and an important parameter is isolation between the beams. In this paper we presented multibeam patterns with up to 2-dB variations in peak main beam power as the beam is scanned to 45° off boresite. The isolation between the receivers for two signal sources was measured. Namely, each receiver preferentially receives from one of the sources, but some signal from the other source is also present, and referred to as the "crosstalk" signal. The relative amount of the crosstalk depends on the spatial separation between the sources and is shown from the measurements presented in this paper to be better than 30 dB for receivers that correspond to incident beams 15° apart. The lens arrays therefore have angle diversity properties which allow them not only to reduce effects of fading, but make them attractive for use in smart antennas with angle-of-arrival detection at the front end, relieving the load on processing circuitry.

Acknowledgment

Z. Popovic would like to thank the German Alexander von Humboldt Stiftung for funding under a Humboldt Research Award for Senior U.S. Scientists.

References

[1] W. C. Jakes, Ed., *Microwave Mobile Communications*. Piscataway, NJ: IEEE Press, 1994.
[2] W. L. Stutzman, J. H. Reed, C. B. Dietrich, B. K. Kim, and D. G. Sweeney, "Recent results from smart antenna experiments—base station and handheld terminals," in *Proc. RAWCON*, Sept. 2000, pp. 139–142.
[3] P. L. Perini and C. L. Holloway, "Angle and space diversity comparisons in different mobile radio environments," *IEEE Trans. Antennas Propagat.*, vol. 46, pp. 764–775, June 1998.
[4] B. S. Collins, "Polarization diversity antennas for compact base stations," *Microwave J.*, vol. 43, pp. 76–88, Jan. 2000.
[5] C. Beckman and U. Wahlberg, "Antenna systems for polarization diversity," *Microwave J.*, vol. 40, no. 5, pp. 330–334, May 1997.
[6] S. Hollung, A. Cox, and Z. Popovic, "A quasioptical bi-directional lens amplifier," *IEEE Trans. Microwave Theory Techniques*, vol. 47, pp. 2352–2357, Dec. 1997.
[7] Z. Popovic and A. Mortazawi, "Quasioptical transmit/receive front ends," *IEEE Trans. Microwave Theory Tech.*, vol. 48, pp. 1964–1975, Nov. 1998.
[8] D. Z. Anderson, V. Damiao, E. Fotheringham, D. Popovic, S. Romisch, and Z. Popovic, "Optically smart active antenna arrays," in *Proc. IEEE 2000 IMS Dig.*, Boston, MA, June 2000, pp. 843–846.
[9] J. Vain and Z. Popovic, "Smart lens antenna arrays," in *Proc. IEEE 2001 IMS Symp. Dig.*, Phoenix, AZ, May 2001, pp. 129–132.
[10] D. T. McGrath, "Planar three-dimensional constrained lenses," *IEEE Trans. Antennas Propagat.*, vol. AP-34, pp. 46–50, Jan. 1986.
[11] A. M. Sayeed, "On modeling multi-antenna multipath channels," in *Proc. 38th Annu. Allerton Conf. Dig.*, Oct. 2000.

Darko Popović received the Dipl. Ing. degree from the University of Belgrade, Serbia, Yugoslavia in 1995. He is currently working toward the Ph.D. degree in electrical engineering at the University of Colorado, Boulder.

From 1995 to 1998, he was a Research Assistant at the Institute of Physics, Belgrade, Yugoslavia. He worked at the National Institute of Standards and Technology, Boulder, CO, on the design of a new generation of atomic clock synthesizers on an exchange visitor program in 1998. His research interests include microwave active antennas, microwave communications, and RF photonics.

Zoya Popović (SM'99–F'02) received the Dipl. Ing. degree from the University of Belgrade, Serbia, Yugoslavia, and the Ph.D. degree from California Institute of Technology, Pasadena, in 1985 and 1990, respectively.

Since 1990, she has been a Professor at University of Colorado, Boulder. She is a coauthor of a textbook and workbook entitled *Introductory Electromagnetics* (Englewood Cliffs, NJ: Prentice-Hall, 2000) for which she received the ASEE Hewlett Packard Terman Award in 2001. She is also coeditor of *Active and Quasi-Optical Arrays for Solid-State Power Combining* (New York: Wiley, 1997). Her research interests include microwave active antennas, smart antennas, high-efficiency microwave circuits, quasioptical techniques, rf photonics, receivers for radioastronomy and front ends for communication systems.

Dr. Popovic received the 1993 IEEE MTT Microwave Prize, 1993 URSI Young Scientist and NSF Presidential Faculty Fellow awards, and 1996 URSI Issac Koga Gold Medal. In 1997, she was chosen Professor of the year by *Eta Kappa Nu* students. In 2000, she received a Humboldt Research Award for Senior U.S. Scientists from the German Alexander von Humboldt Foundation.